Bioimaging

Deutsche Ausgabe: DOI: 10.1002/ange.201606285
Internationale Ausgabe: DOI: 10.1002/anie.201606285

An Ultrasensitive Cyclization-Based Fluorescent Probe for Imaging Native HOBr in Live Cells and Zebrafish

*Kehua Xu, Dongrui Luan, Xiaoting Wang, Bo Hu, Xiaojun Liu, Fanpeng Kong, and Bo Tang**

Abstract: *Bromine has been reported recently as being the 28th essential element for human health. HOBr, which is generated in vivo from bromide, is a required factor in the formation of sulfilimine crosslinks in collagen IV. However, to date, no method for the specific detection of native HOBr in vivo has been reported. Herein, we develop a simple small molecular probe for imaging HOBr based on a specific cyclization catalyzed by HOBr. The probe can be easily synthesized in high yield through a Suzuki cross-coupling reaction. The probe exhibits ultrahigh sensitivity at the picomole level, in addition to specificity for HOBr and real-time response. Importantly, without Br^- stimulation, this probe reports native HOBr levels in HepG2 cells. Thus, the probe is a promising new tool for imaging endogenous HOBr and may provide a means for finding new physiological functions of HOBr in living organisms.*

Hypobromous acid (HOBr) has received a great deal of attention owing to its strong oxidizing power and antibacterial action.[1] The excessive generation and accumulation of HOBr in vivo is harmful to organisms and its damaging effects are connected to a wide range of diseases, including rheumatoid arthritis,[2,3] inflammatory tissue damage,[1,4,5] cardiovascular disease,[6–8] neurodegenerative conditions,[6] kidney disease,[9,10] and cancers.[11,12] Recently, B.G. Hudson et al. found that HOBr plays key roles in the formation of sulfilimine crosslinks in collagen IV.[13] Collagen IV scaffolds are critical for the formation and function of basement membranes (BMs) in animals.[14–16] In vivo, HOBr is generated from the peroxidation of the bromide anion (Br^-) with hydrogen peroxide, a reaction catalyzed by a heme peroxidase,[17] such as myeloperoxidase (MPO) or eosinophil peroxidase (EPO).[18,19] To better elucidate the physiological and pathological functions of HOBr, it is necessary to develop suitable probes for endogenous HOBr.

The blood and plasma levels of Br^- are far lower than that of chloride anion (Cl^-) by approximately 1000-fold,[20] which leads to a relatively lower concentration of HOBr than HOCl. Recently, a number of practical fluorescent probes for HOCl have been reported, such as two-photon fluorescent probes that target mitochondria and lysosomes[21] and an enhanced-PET-based ultrasensitive fluorescent probe.[22] However, to the best of our knowledge, no fluorescent probe suitable for the specific detection of HOBr in vivo has been reported, although the reversible detection of HOBr/Vc (ascorbic acid) and HOBr/H_2S were discussed.[23,24] Therefore, it would be a challenge to establish a suitable approach for quantifying endogenous HOBr, because of its low concentration and high activity. Furthermore, it is notable that previous studies have not considered the strict distinction between HOBr and OBr^-.

Inspired by the latest research by B.G. Hudson et al. on the effect of HOBr on crosslink formation in collagen IV,[13] we have designed a sulfilimine-based fluorescent probe for the specific detection of HOBr. The simple synthetic strategy is shown in Scheme 1. The biphenyl probe (**BPP**) can be directly synthesized using commercially available *o*-bromoaniline and *o*-(methylthio)-phenylboronic acid in high yield. In the presence of HOBr, a rapid cyclization reaction occurs between the amino group and *S*-methyl group of the probe molecule, thus generating a product with a red-shifted emission. This red-shift is extremely important for the method because it ensures that the fluorescence of the unreacted probe will not interfere with the measurement. Our probe was easily synthesized in 85 % yield, and the maximum excitation and emission wavelengths of the probe are 375 and 435 nm, respectively, whereas those of the reaction product are 480 and 525 nm. A rapid response to HOBr was observed for the probe with high selectivity and ultrasensitivity, and the proposed reaction mechanism is shown in Scheme 2. Importantly, neither Br^- nor H_2O_2 could affect the fluorescence intensity of the probe in simulated physiological conditions, but HepG2 cells and zebrafish treated with Br^-, Br^-/H_2O_2, or HOBr showed different intensities of fluorescence emission, which revealed a relationship between HOBr and Br^-/H_2O_2 in vivo. Thus, this probe should be a promising tool for quantifying endogenous HOBr and could provide a means of finding new functions of HOBr and aid in studying the interconversion of Br^-, Br^-/H_2O_2, and HOBr in living

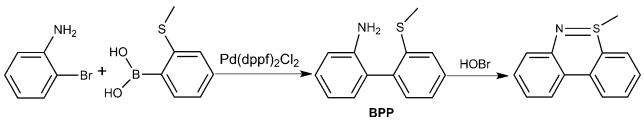

Scheme 1. Synthesis of the probe (**BPP**) and its response to HOBr.

[*] Prof. K. Xu, Dr. D. Luan, Dr. X. Wang, Dr. B. Hu, Dr. X. Liu, Dr. F. Kong, Prof. B. Tang
College of Chemistry, Chemical Engineering and Materials Science, Collaborative Innovation Center of Functionalized Probes for Chemical Imaging in Universities of Shandong, Key Laboratory of Molecular and Nano Probes, Ministry of Education, Shandong Provincial Key Laboratory of Clean Production of Fine Chemicals, Shandong Normal University
Jinan 250014 (P.R. China)
E-mail: tangb@sdnu.edu.cn

Supporting information for this article can be found under: http://dx.doi.org/10.1002/anie.201606285.

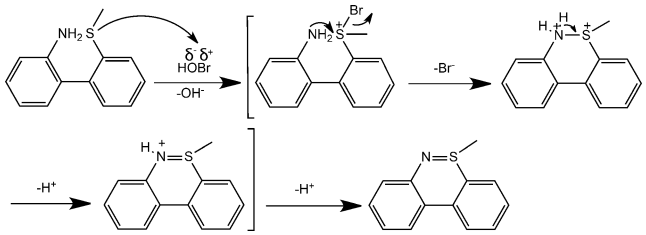

Scheme 2. The proposed mechanism for the response of **BPP** to HOBr.

organisms. We expect that **BPP** will be widely used as a commercial reagent.

The probe was synthesized as shown in Scheme 1, and the structures of **BPP** and the reaction product of **BPP** with HOBr were fully characterized by HRMS, ^{1}H NMR, and ^{13}C NMR, and a titration experiment of BPP with HOBr based on ^{1}H NMR was performed (see Supporting Information, Section S2, S3 and S14). The fluorescence properties of the probe and reaction product were also investigated, as shown in Figure 1 a. A large red shift in the maximum emission wavelength (ca. 100 nm) was observed under simulated physiological conditions, which improves the detection sensitivity.

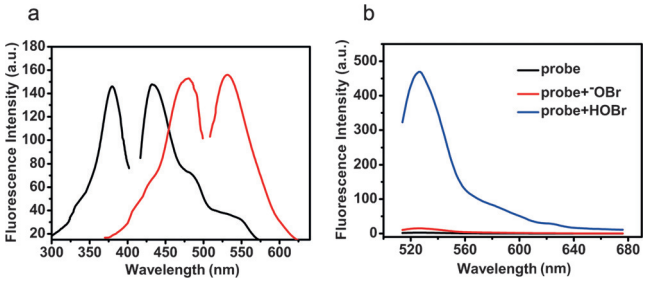

Figure 1. a) Excitation and emission spectra of the probe (black) and the product of the probe with HOBr (red). b) The fluorescence response of the probe (5 μM) toward HOBr (20 μM) or NaOBr (500 μM) in ultrapure water. Slit widths: 10/10 nm. $\lambda_{ex}/\lambda_{em}$ = 480/525 nm.

Previous reports have suggested that the molecular mechanism during the HOCl oxidation of sulfide-type amino acids is an electrophilic addition reaction triggered by chloronium ions (Cl^+) rather than ^-OCl.[25,26] Additionally, B.G. Hudson et al. proposed that Br^+ from HOBr catalyzes the coupling reaction of an amino group with an *S*-methyl group to form a S=N bond in collagen IV.[13] Herein, we first tested the responses of the probe to HOBr and NaOBr in ultrapure water. As shown in Figure 1 b, our probe is able to recognize HOBr but not ^-OBr, which suggests that the proposed HOBr detection mechanism given in Scheme 2 for our probe is reasonable. Next, the response of **BPP** to HOBr was tested under different conditions, including pH values ranging from 2.0 to 12.0 (Supporting Information, Figure S1) and **BPP** concentrations ranging from 1 nM to 20 μM (Supporting Information, Figure S2). The fluorescence resulting from the reaction of **BPP** with HOBr does not change over a wide pH range, and the changes are especially negligible between pH values of 6.0 and 8.0. The responses of the probe (5 μM) to various concentrations of HOBr were measured at pH 7.4 (Figure 2 a,b), and a linear relationship was observed between the fluorescence intensity and HOBr concentrations

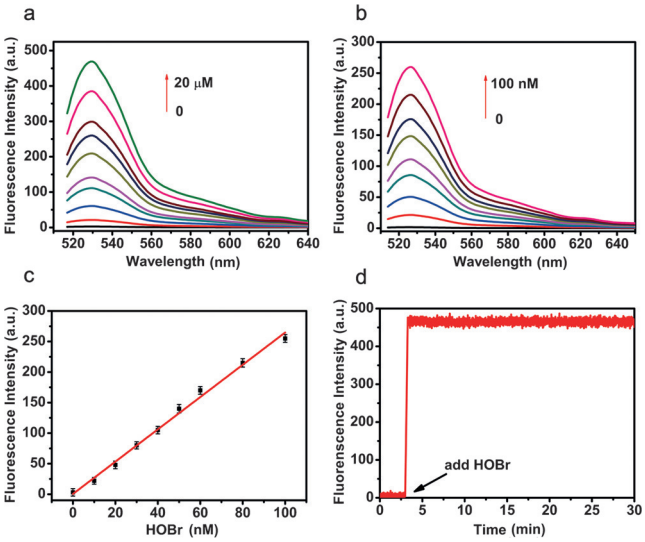

Figure 2. a) Fluorescence spectra of the probe (5 μM) toward various concentrations of HOBr (0–20 μM) in PBS (10 mM, pH 7.4, 0.5% CH_3CN as a cosolvent). Slit widths: 10/ 10 nm. b) Fluorescence spectra of the probe (5 μM) with various concentrations of HOBr (0–100 nM) in PBS (10 mM, pH 7.4). Slit widths: 20/ 20 nm. c) The linear relationship between fluorescence intensity and HOBr concentrations in the range from 0 to 100 nM. d) Time course of the fluorescence intensities of 5 μM **BPP** with 20 μM HOBr in PBS (10 mM, pH 7.4). Voltage: 600 V. Slit widths: 10/10 nm. $\lambda_{ex}/\lambda_{em}$ = 480/525 nm.

from 0 to 100 nM (Figure 2 c). The regression equation was $F = 0.48 + 2.64\,[HOBr]$ nM, with a linear coefficient of 0.9960. The detection limit (3S/m) was determined to be 17 pM, which is sufficient to image endogenous HOBr (20–100 μM in plasma[27]). Obviously, the ultrasensitivity of the probe is due to the fast cyclization of the amino group and *S*-methyl group of **BPP** catalyzed by HOBr to generate a high-quantum-yield product ($\Phi_F = 0.31$, see Supporting Information, Section S10) with a large red-shift in emission. The large red-shift in emission wavelength greatly improves the signal-to-noise ratio of the detection signal. Finally, the reaction kinetics of **BPP** with HOBr in phosphate-buffered saline (PBS, 10 mM, pH 7.4) was analyzed. As shown in Figure 2 d, the method allows the real-time determination of HOBr, which is important for accurately quantifying highly active species.

Next, we studied the selectivity of the probe to HOBr. The potential interfering species were classified into two groups: highly active oxidizing species and active reducing species. Figure 3 a shows that the probe did not display a significant fluorescence increase in the presence of other reactive oxygen species (ROS), including H_2O_2, *t*-BuOOH, $ONOO^-$, O_2^-, $^1O_2$, $^{\bullet}OH$, NO, or even HOCl. It was interesting for us to see this difference between HOBr and HOCl in the coupled reaction of the amino group and *S*-methyl group (Supporting

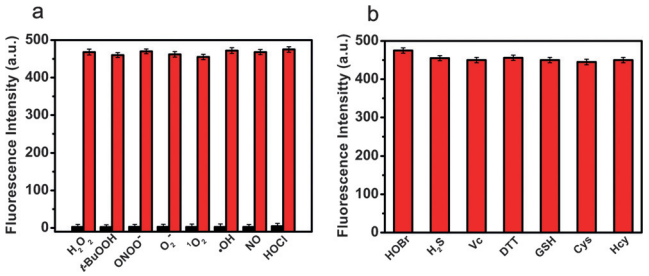

Figure 3. a) Fluorescence intensity of the probe after adding active oxidizing species. Black bars show the addition of one of these interferents to a solution of 5 μM **BPP**. The red bars represent the addition of both HOBr and one interferent to the probe solution. 500 μM each for H_2O_2, *t*-BuOOH, $ONOO^-$, O_2^-, $^1O_2$, ·OH, and NO; 200 μM for HOCl; and 20 μM for HOBr. b) Fluorescence intensity of the reaction product of the probe with HOBr after adding active reducing species. 500 μM for GSH; 300 μM each for Cys and Hcy; 150 μM for Vc; 200 μM for DTT; and 80 μM for H_2S. Slit widths: 10/10 nm. $\lambda_{ex}/\lambda_{em} = 480/525$ nm.

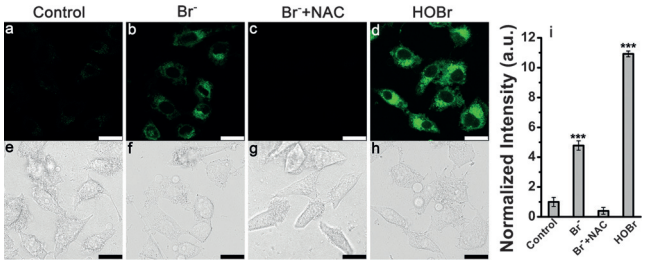

Figure 4. Confocal fluorescence imaging of intracellular HOBr in HepG2 cells. a) HepG2 cells incubated with **BPP** (50 μM) for 30 min; b) HepG2 cells first incubated with **BPP** (50 μM) for 30 min and then incubated with NaBr (100 μM) for 30 min; c) same as (a) and then incubated with NaBr (100 μM) and NAC (10 μM) for 30 min; d) same as (a) and then incubated with HOBr (100 μM) for 30 min. e)–h) Brightfield images of (a)–(d). i) Normalized fluorescence intensity of cells in panels (a)–(d). The cell images shown are representative ($n = 10$ fields of cells). Fluorescence images were acquired using a confocal microscope with 488 nm excitation and 500–600 nm collection. Data are presented as the mean ± SEM; $^{***}p < 0.001$ versus control group cells. The results are representative of three independent experiments. Scale bar = 25 μm.

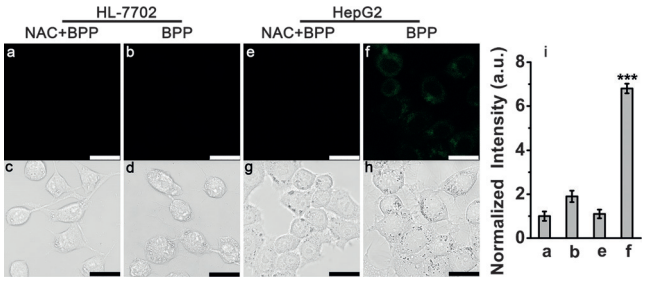

Figure 5. Fluorescence imaging of native HOBr. a) HL-7702 cells incubated with NAC (10 μM) for 30 min and then with **BPP** (50 μM) for 30 min; b) HL-7702 cells incubated with probe (50 μM) for 30 min; c)–d) bright-field images of HL-7702 cells; e) HepG2 cells incubated with NAC (10 μM) for 30 min and then with **BPP** (50 μM) for 30 min; f) HepG2 cells incubated with probe (50 μM) for 30 min; g)–h) bright-field images of HepG2 cells. i) Normalized fluorescence intensity of cells in panels (a), (b), (e), and (f). The provided images of cells are representative ($n = 10$ fields of cells). Fluorescence images were acquired at 488 nm excitation and 500–600 nm emission wavelengths. Data are presented as the mean ± SEM; $^{***}p < 0.001$ versus group (b) cells. Results are representative of three independent experiments. Scale bar = 25 μm.

Information, Scheme S1 and Figure S3). Figure 3b shows that the fluorescence responses of the probe to HOBr were hardly affected by the presence of H_2S, vitamin C (Vc), dithiothreitol (DTT), GSH, Cys, or Hcy, which confirmed that the reaction product of **BPP** and HOBr is stable in complex environments. Additionally, the responses of **BPP** toward metal ions and amino acids were examined under the same conditions (Supporting Information, Figures S4 and S5). In short, the probe possesses excellent selectivity for HOBr over possible interfering species derived from living cells, which suggests that it would be useful for imaging HOBr in vitro and in vivo.

To test the ability of the probe to image HOBr in biological systems, we first studied the cytotoxicity of the probe and the photostability of the reaction product. The MTT assays were performed in HepG2 cells (Supporting Information, Figure S6). The IC_{50} value was 711.20 μM, suggesting that the probe has low toxicity towards living cells. Photostability tests showed that the reaction product of **BPP** with HOBr in HepG2 cells is highly resistant to photobleaching (Supporting Information, Figure S7). After confirming the sensitivity, selectivity, cytotoxicity, and photostability of the probe or product, we explored the potential of **BPP** for imaging HOBr in vitro. Probe-treated HepG2 cells were divided into four groups and incubated in Dulbecco's modified Eagle's medium (DMEM) containing PBS, NaBr, NaBr and NAC (*N*-acetyl-L-cysteine, a scavenger of HOBr), or HOBr. After 30 min, fluorescence images were obtained (Figure 4). The results show that the Br^--stimulated cells and the HOBr-treated cells displayed strong fluorescence and the fluorescence enhancement can be largely inhibited by NAC. This demonstrates that **BPP** is capable of monitoring the generation of endogenous HOBr in HepG2 cells. Moreover, a weak fluorescence signal was observed in HepG2 cells treated with PBS only (Figure 4a,i), which suggests that native HOBr could also be monitored. Subsequently, imaging of native HOBr was carried out by pretreating cells with NAC and comparing them to untreated cells (Figure 5). The results show that a brighter fluorescence signal was detected from HepG2 cells than from HL-7702 cells, and a similar fluorescence-inhibiting effect by NAC was observed in HepG2 and HL-7702 cells, further supporting the idea that the fluorescence of untreated cells incubated with **BPP** arises from the action of native HOBr. Additionally, a close relationship between Br^-, H_2O_2 and HOBr was verified when probe-treated cells were incubated with Br^-, Br^- and H_2O_2, or HOBr, as shown in the Supporting Information, Figure S8. The result shows that HOBr can be generated by the peroxidation of bromide anion (Br^-) with hydrogen peroxide in living cells.

Finally, we explored the potential of the probe as an in vivo imaging tool. In these experiments, different developmental stages of zebrafish embryos were used. Briefly, 48, 72, and 120 hpf (hours postfertilization) zebrafish embryos

were each divided into two groups, each having 10 embryos. The embryos in a control group were only fed the probe for 30 min, and the embryos in the other group were pretreated with NaBr or NAC for 30 min, and then fed with the probe for 30 min. NAC was used to eliminate endogenous HOBr. Fluorescence images were collected using scanning confocal microscopy, as shown in Figure 6. The zebrafish embryos that were fed Br^- emitted brighter fluorescence than those that

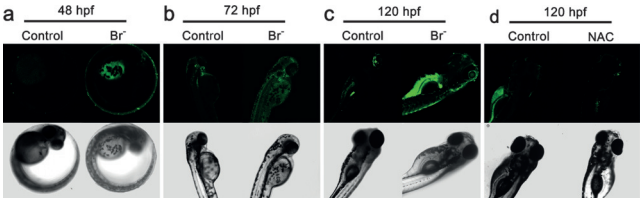

Figure 6. In vivo fluorescence imaging of HOBr in zebrafish at three different developmental stages. a) 48 hpf (hours past fertilization), b) 72 hpf, c) 120 hpf and d) elimination of endogenous HOBr with NAC. In all cases, the embryos in the control group were only fed the probe for 30 min, whereas the embryos in the other group were pretreated with Br^- (100 μM) or NAC (10 μM) for 30 min and then fed with the probe for 30 min. The embryo images shown are representative ($n = 10$ fields of embryos). The results are representative of three independent experiments. Scale bar = 250 μm.

were not fed Br^-, while those embryos pretreated with NAC displayed the lowest fluorescence. These results further confirmed that HOBr can be generated from Br^- in living organisms[13] and the native HOBr can be measured by **BPP**. Therefore, we believe that the probe is a promising tool for monitoring changes in HOBr levels in vivo.

In conclusion, we have developed an ultrasensitive fluorescence probe for detecting hypobromous acid in vitro and in vivo. The probe is easily synthesized in high yield and exhibits a real-time response to HOBr with specificity and ultrasensitivity (picomole level). The imaging of endogenous HOBr in HepG2 cells and zebrafish can be performed using the probe. Moreover, the probe reports native HOBr levels in HepG2 cells without bromine anion stimulation. Therefore, this probe is a promising tool for monitoring changes in HOBr levels in vivo and paves the way for acquiring new insight into the physiological action of HOBr.

Acknowledgements

This work was supported by the 973 Program (2013CB933800) and the National Natural Science Foundation of China (21535004, 21227005, 21390411, 21275092, 21575081, and 21507075).

Keywords: bioimaging · cyclization reactions · fluorescent probes · hypobromous acid

How to cite: *Angew. Chem. Int. Ed.* **2016**, *55*, 12751–12754
Angew. Chem. **2016**, *128*, 12943–12946

[1] A. Lane, J. Tan, C. Hawkins, A. Heather, M. Davies, *Biochem. J.* **2010**, *430*, 161–169.
[2] J. J. Hu, N. K. Wong, S. Ye, X. Chen, M. Y. Lu, A. Q. Zhao, Y. Guo, A. C. Ma, A. Y. Leung, J. Shen, D. Yang, *J. Am. Chem. Soc.* **2015**, *137*, 6837–6843.
[3] D. L. Longo, S. L. Archer, *N. Engl. J. Med.* **2013**, *369*, 2236–2251.
[4] M. J. Ceko, K. Hummitzsch, N. Hatzirodos, W. Bonner, S. A. James, J. K. Kirby, R. J. Rodgers, H. H. Harris, *Metallomics* **2015**, *7*, 756–765.
[5] J. C. van Dalen, W. M. Whitehouse, C. C. Winterbourn, J. A. Kettle, *Biochem. J.* **1997**, *327*, 487–492.
[6] Y. W. Yap, M. Whiteman, N. S. Cheung, *Cell. Signalling* **2007**, *19*, 219–228.
[7] S. Sugiyama, Y. Okada, G. K. Sukhova, R. Virmani, J. W. Heinecke, P. Libby, *Am. J. Pathol.* **2001**, *158*, 879–891.
[8] M. J. Steinbeck, L. J. Nesti, P. F. Sharkey, J. Parvizi, *J. Orthop. Res.* **2007**, *25*, 1128–1135.
[9] K. L. Brown, C. Darris, K. L. Rose, O. A. Sanchez, H. Madu, J. Avance, N. Brooks, M. Zhang, A. Fogo, R. Harris, *Diabetes* **2015**, *64*, 2242–2253.
[10] V. M. Monnier, *Diabetes* **2015**, *64*, 1910–1911.
[11] R. A. Cairns, I. S. Harris, T. W. Mak, *Nat. Rev. Cancer* **2011**, *11*, 85–95.
[12] C. Gorrini, I. S. Harris, T. W. Mak, *Nat. Rev. Drug Discovery* **2013**, *12*, 931–947.
[13] A. S. McCall, C. F. Cummings, G. Bhave, R. Vanacore, A. Page-McCaw, B. G. Hudson, *Cell* **2014**, *157*, 1380–1392.
[14] R. Vanacore, A. J. Ham, M. Voehler, C. R. Sanders, T. P. Conrads, T. D. Veenstra, K. B. Sharpless, P. E. Dawson, B. G. Hudson, *Science* **2009**, *325*, 1230–1234.
[15] K. Kühn, *Matrix Biol.* **1995**, *14*, 439–445.
[16] A. L. Fidler, R. M. Vanacore, S. V. Chetyrkin, V. K. Pedchenko, G. Bhave, V. P. Yin, C. L. Stothers, K. L. Rose, W. H. McDonald, T. A. Clark, D. B. Borza, R. E. Steele, M. T. Ivy, J. K. Hudson, B. G. Hudson, *Proc. Natl. Acad. Sci. USA* **2014**, *111*, 331–336.
[17] W. Wu, Y. Chen, A. D'Avignon, S. L. Hazen, *Biochemistry* **1999**, *38*, 3538–3548.
[18] C. J. van Dalen, A. J. Kettle, *Biochem. J.* **2001**, *358*, 233–239.
[19] P. G. Furtmüller, U. Burner, G. Regelsberger, C. Obinger, *Biochemistry* **2000**, *39*, 15578–15584.
[20] V. F. Ximenes, N. H. Morgon, A. R. de Souza, *J. Inorg. Biochem.* **2015**, *146*, 61–68.
[21] L. Yuan, L. Wang, B. K. Agrawalla, S. J. Park, H. Zhu, B. Sivaraman, J. Peng, Q. H. Xu, Y. T. Chang, *J. Am. Chem. Soc.* **2015**, *137*, 5930–5938.
[22] H. Zhu, J. Fan, J. Wang, H. Mu, X. Peng, *J. Am. Chem. Soc.* **2014**, *136*, 12820–12823.
[23] F. Yu, P. Song, P. Li, B. Wang, K. Han, *Chem. Commun.* **2012**, *48*, 7735–7737.
[24] B. Wang, P. Li, F. Yu, J. Chen, Z. Qu, K. Han, *Chem. Commun.* **2013**, *49*, 5790–5792.
[25] P. Nagy, M. T. Ashby, *Chem. Res. Toxicol.* **2005**, *18*, 919–923.
[26] X. L. Armesto, M. Canle, M. I. Fernández, M. V. Garcia, J. A. Santaballa, *Tetrahedron* **2000**, *56*, 1103–1109.
[27] J. P. Gaut, G. C. Yeh, H. D. Tran, J. Byun, J. P. Henderson, G. M. Richter, M. L. Brennan, A. J. Lusis, A. Belaaouaj, R. S. Hotchkiss, J. W. Heinecke, *Proc. Natl. Acad. Sci. USA* **2001**, *98*, 11961–11966.

Received: June 28, 2016
Revised: August 3, 2016
Published online: September 15, 2016